

Phase Equilibria and Crystal Chemistry of Rubidium Niobates and Rubidium Tantalates*

D. B. Minor, R. S. Roth, H. S. Parker, and W. S. Brower

Institute for Materials Research, National Bureau of Standards, Washington, D.C. 20234

(August 2, 1977)

The phase equilibria relations and crystal chemistry of portions of the $\text{Rb}_2\text{O}-\text{Nb}_2\text{O}_5$ and $\text{Rb}_2\text{O}-\text{Ta}_2\text{O}_5$ systems were investigated for structures potentially useful as ionic conductors. A hexagonal tungsten bronze-type (HTB) structure was found in both systems as well as three hexagonal phases with mixed HTB-pyrochlore type structures. Ion exchange experiments between various alkali ions are described for several phases. Unit cell dimensions and x-ray diffraction powder patterns are reported.

Key words: Crystal chemistry; ionic conductivity; non-stoichiometry; phase equilibria; rubidium niobate; rubidium tantalate.

1. Introduction

Research in this laboratory in the alkali niobate and tantalate systems has been conducted for the purpose of determining the phase equilibria diagrams of these systems and to observe if structures were present which might be favorable as ionic conductors [1, 2].¹ In this paper the results of the study of portions of the $\text{Rb}_2\text{O}-\text{Nb}_2\text{O}_5$ and $\text{Rb}_2\text{O}-\text{Ta}_2\text{O}_5$ systems will be presented. Discussion of the remaining alkali niobate and alkali tantalate systems will be published later.

The phase equilibria relations in the $\text{Rb}_2\text{O}-\text{Nb}_2\text{O}_5$ system were first studied by Riesman and Holtzberg [3]. On the basis of unindexed x-ray diffraction patterns and density determinations, the compositions of 8 observed phases were reported. These have the molar ratios, $\text{Rb}_2\text{O}:\text{Nb}_2\text{O}_5$, of 2:15 (11.75 mol per cent Rb_2O), 1:4, 4:11 (26.67 mol per cent Rb_2O), 1:2, 2:3, 1:1, 4:3 (57.14 mol per cent Rb_2O), and 4:1.

Iyer and Smith [4] reported the preparation of phases suggested to have the molar ratios, $\text{Rb}_2\text{O}:\text{Nb}_2\text{O}_5$, 2:3, 1:2, 1:3 (Riesman and Holtzberg's 4:11), 1:4, and 1:13 (Riesman and Holtzberg's 2:15). In the Ta_2O_5 rich portion of the $\text{Rb}_2\text{O}-\text{Ta}_2\text{O}_5$ system the only compound that was found by Iyer and Smith [4] was RbTa_3O_8 . Gatehouse et al. [5] reported the unit cell dimensions and partial structure determinations of two of the niobate phases. One of these, " RbNb_3O_9 ", was reported to have a hexagonal tungsten bronze-type (HTB) structure and the other, " $\text{Rb}_3\text{Nb}_{54}\text{O}_{146}$ ", had a new tetragonal structure with 7-sided tunnels called, in this paper, a Gatehouse tetragonal-bronze (GTB).

2. Methods and Results

2.1. The System $\text{Rb}_2\text{O}:\text{Nb}_2\text{O}_5$

The system $\text{Rb}_2\text{O}:\text{Nb}_2\text{O}_5$ was investigated from the region of 73.33 to 100 mol per cent Nb_2O_5 . Ten compositions were prepared by dry mixing Rb_2CO_3 and Nb_2O_5 and calcining in

open Pt crucibles at 500 °C for 120 hours and 600 °C for 90 hours with intermediate grindings. Portions from each composition were heated at higher temperatures in sealed Pt tubes in resistance wound quench-type furnaces and quenched into water. Temperature was measured with a 100 Pt/90 Pt-10 Rh thermocouple calibrated against the melting points of gold and palladium, 1064 and 1554 °C, respectively [6]. The temperatures reported are considered to be accurate ± 5 °C, up to 1500 °C. Samples were identified at room temperature by x-ray powder diffraction using Ni-filtered Cu radiation and a $1/4^\circ 2\theta/\text{min}$ scanning rate. X-ray diffraction powder patterns of the quenched specimens were used to establish the phase equilibrium diagram shown in figure 1.

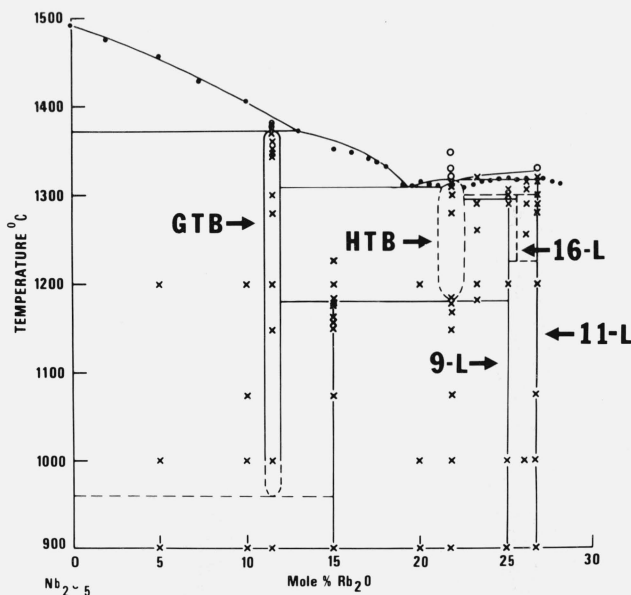


FIGURE 1. Phase diagram for the system $\text{Nb}_2\text{O}_5:4\text{Rb}_2\text{O}:11\text{Nb}_2\text{O}_5$.

* This research was partially supported by NASA-Lewis Research Center Contract C-50821-C.

¹ Figures in brackets indicate the literature references at the end of this paper.

Table 1 details the experimental data for this system. Only the x-ray diffraction pattern of the phase occurring at low temperature at about 15 mol per cent Rb_2O has not been indexed. No single crystals of this phase were obtained.

Table 1. Experimental Data for the System $\text{Nb}_2\text{O}_5\text{-}4\text{Rb}_2\text{O:}11\text{Nb}_2\text{O}_5$.

Composition	Previous Heat Treatment		Final Heat ^a / Treatment		Results of Physical Observation	Results of X-ray Diffraction Analysis
	Temp. °C	Time hr	Temp. °C	Time hr		
$5\text{Rb}_2\text{O:}95\text{Nb}_2\text{O}_5$	500 500 600	120 120 90	500	120 ^b /		$\text{H-Nb}_2\text{O}_5 + 2:3$
			600	90 ^b /		$\text{H-Nb}_2\text{O}_5 + 3:17$
			800	66		$\text{H-Nb}_2\text{O}_5 + 3:17$
			900	40		$\text{H-Nb}_2\text{O}_5 + 3:17$
			1000	80		$\text{H-Nb}_2\text{O}_5 + 3:17$
			1000	111 ^c /		
			1200	88		$\text{H-Nb}_2\text{O}_5 + \text{GTB}$
$10\text{Rb}_2\text{O:}90\text{Nb}_2\text{O}_5$	500 500 600	120 120 90	500	120 ^b /		$\text{H-Nb}_2\text{O}_5 + 2:3$
			600	90 ^b /		$\text{H-Nb}_2\text{O}_5 + 2:3$
			800	60		$3:17 + \text{H-Nb}_2\text{O}_5$
			900	40		$3:17 + \text{H-Nb}_2\text{O}_5$
			1000	80		$3:17 + \text{GTB} + \text{H-Nb}_2\text{O}_5$
			1000	111 ^c /		$\text{GTB} + 3:17 + \text{H-Nb}_2\text{O}_5$
			1075	60		$\text{GTB} + \text{H-Nb}_2\text{O}_5$
			1200	88		$\text{GTB} + \text{H-Nb}_2\text{O}_5$
			500	120 ^b /		$\text{H-Nb}_2\text{O}_5 + 2:3$
			600	90 ^b /		$\text{H-Nb}_2\text{O}_5 + 2:3$
$11.5\text{Rb}_2\text{O:}88.5\text{Nb}_2\text{O}_5$	500 500 600	120 120 90	500	120 ^b /		$\text{H-Nb}_2\text{O}_5 + 2:3$
			600	90 ^b /		$\text{H-Nb}_2\text{O}_5 + 2:3$
			800	60		$3:17 + \text{H-Nb}_2\text{O}_5$
			900	40		$3:17 + \text{H-Nb}_2\text{O}_5$
			1000	80		$\text{GTB} + 3:17$
			1000	111 ^c /		$\text{GTB} + 3:17$
			1000	111 ^c /		$\text{GTB} + 3:17$
			500	120		
			600	90		
			1000	111		
			1148	16		GTB
			1200	88		GTB
			1280	40		GTB
			1340	1.5	Not melted	
			1349	23		GTB
			1352	.25	Not melted	
			1355	.33	Not melted	
			1361	1	Not melted	
			1369	.5	Not melted	
			1375	1.5	Partial melted	GTB
			1380	2	Completed melted	
$15\text{Rb}_2\text{O:}85\text{Nb}_2\text{O}_5$	500 500 600	120 120 90	500	120 ^b /		$\text{H-Nb}_2\text{O}_5 + 2:3$
			600	90 ^b /		$\text{H-Nb}_2\text{O}_5 + 2:3$
			750	16 ^c /		$11\text{-L} + \text{H-Nb}_2\text{O}_5$
			750	16 ^d /		$3:17$
			800	66		$3:17$
			900	40		$3:17$
			1000	80		$3:17$
			1000	111 ^c /		$3:17$
			1075	60		$3:17$
			1200	88		$\text{GTB} + \text{HTB}$
			500	120		
			600	90		
			1000	111		
			1200	16.5		
			1156	16.5		$3:17$
			1177	24		$3:17 + \text{GTB}$
			1180	23		$3:17 + \text{GTB}$
			1183	64		$\text{HTB} + \text{GTB}$
			1226	18		$\text{HTB} + \text{GTB}$
			1262	18		--
			1349	23		$\text{HTB} + \text{GTB}$
$20\text{Rb}_2\text{O:}80\text{Nb}_2\text{O}_5$	500 500 600	120 120 90	500	120 ^b /		$\text{H-Nb}_2\text{O}_5 + 2:3$
			600	90 ^b /		$\text{H-Nb}_2\text{O}_5 + 2:3$
			800	66		$3:17 + 11\text{-L}$
			900	40		$3:17 + 11\text{-L}$
			1000	80		$3:17 + 11\text{-L}$
			1000	111 ^c /		
			1200	88		$9\text{L} + \text{GTB} + \text{HTB}$
			500	120 ^b /		
			600	90 ^b /		
			1153	84 ^b /		$\text{GTB} + 3:17$
			1153	84 ^b /		$\text{GTB} + 3:17$
$21.75\text{Rb}_2\text{O:}78.25\text{Nb}_2\text{O}_5$	500 500 600	120 120 90	500	120 ^b /		$\text{H-Nb}_2\text{O}_5 + 2:3$
			600	90 ^b /		$\text{H-Nb}_2\text{O}_5 + 2:3$
			800	66		$3:17 + 11\text{-L}$
			900	40		--
			1000	80		$3:17 + 9\text{-L} + 11\text{-L}$
			1000	111 ^c /		--
			1075	60		$3:17 + 9\text{-L}$
			1200	88		$9\text{-L} + \text{GTB}$
			1241	18		$\text{HTB} + 9\text{-L}$
			1250	16		$\text{HTB} + 9\text{-L}$
			1280	?		$\text{HTB} + 9\text{-L}$
			1300	16.5		$\text{HTB} + 11\text{-L} + 16\text{-L}$

Table 1. Experimental Data for the System $\text{Nb}_2\text{O}_5\text{-}4\text{Rb}_2\text{O:}11\text{Nb}_2\text{O}_5$. (cont.)

	500	120				
	600	90				
	1000	111				
			1149	23		9-L + 3:17
			1169	18		9-L + 3:17
			1181	89		9-L + GTB
			1184	3.5		HTB + 9-L
			1313	64		HTB + 11-L
			1315	0.5	Not melted	
			1320	0.5	Partially melted	HTB + 11-L
			1320	22	Completely melted	HTB + 11-L
			1328	1.5	Completely melted	
			1347	16.5	Completely melted	
23.19Rb ₂ O:76.81Nb ₂ O ₅						
	1000	63 ^{c/}				
			1200	21 ^{c/}		9-L + HTB
			1255	18		9-L + HTB
			1290	18.5		9-L + HTB
			1306	22		9-L + HTB
						HTB + 11-L
25Rb ₂ O:75Nb ₂ O ₅			500	120 ^{b/}		Nb ₂ O ₃ + 2:3
	500	120	600	90 ^{b/}		Nb ₂ O ₃ + 2:3
	500	120				
	600	90				
			800	66		11-L + 3:17
			900	40		
			1000	80		11-L + 9-L
			1000	111 ^{c/}		
			1200	88		9-L
			1280	?		9-L + HTB
			1300	40		9-L
	500	120				
	600	90				
	1000	111				
			1290	18.5		--
			1300	16.5		11-L + HTB
25.5Rb ₂ O:74.5Nb ₂ O ₅			500	63 ^{b/}		
	500	63	600	24 ^{b/}		
	500	63				
	600	24				
			1000	69 ^{c/}		9-L + 11-L
			1249	22		9-L
			1258	67		9-L + 16-L
			1262	16		9-L + 16-L
			1265	17		9-L + 16-L
			1275	117		16-L + ?tr
			1284	41		16-L + ?tr
			1285	18		16-L + 11-L
			1287	67		16-L + 11-L
			1291	21		16-L + 11-L
			1294	16		16-L + 11-L
			1297	22		16-L + 11-L
26.67Rb ₂ O:73.33Nb ₂ O ₅			500	120 ^{b/}		H-Nb ₂ O ₅ + 2:3
	500	120	600	90 ^{b/}		H-Nb ₂ O ₅ + 2:3
	500	120				
	600	90				
			750	60		11-L
			800	66		11-L
			900	40		11-L
			1000	80		11-L
			1000	111 ^{c/}		11-L
			1075	60		11-L
			1200	88		11-L
			1241	18		11-L
			1280	40		11-L
			1300	40		H-L
	500	120				
	500	90				
	1000	111				
			1290	18.5		11-L
			1306	22		11-L
			1316	0.5	Not melted	
			1316	16	Partially melted	
			1320	0.5	Partially melted	
			1330	1.5	Completely melted	

^{a/} Except as indicated by a footnote the samples were quenched into water from the temperature indicated.^{b/} The samples were calcined in open Pt crucibles and pulled from the furnaces at the temperatures indicated. Rb₂O may have been volatilized during these calcines thereby changing the composition to one greater in mole percent Nb₂O₅.^{c/} The sample was in a large sealed Pt tube and pulled from the furnace at the temperature and cooled rapidly on a chill block.^{d/} The sample was removed from the furnace at the temperature indicated and immediately dunked into a beaker of water.

This phase can be identified by its major diffraction peaks occurring at $d = 6.92, 3.97, 3.92, 3.54, 3.44, 3.27, 3.16, 2.779$, and 2.472 Å. X-ray powder diffraction patterns of all other phases are given in tables 2–6. Intensities listed in

Table 2

X-ray Diffraction Powder Pattern of the "Gatehouse-Tetragonal-Bronze"-Like Phase Occurring at the Composition $11.5\text{Rb}_2\text{O} \cdot 88.5\text{Nb}_2\text{O}_5$.^{a/}

d_{obs}	hkl	$2\theta_{\text{obs}}$	$2\theta_{\text{calc}}$	I_{obs}
19.53	110	4.52	4.54	5
13.82	200	6.39	6.43	7
12.34	210	7.16	7.19	6
9.72	220	9.09	9.09	8
8.71	310	10.15	10.17	8
7.64	320	11.58	11.60	9
6.67	410	13.27	13.27	6
3.964	001	22.41	22.40	100
3.886	111	22.87	22.87	11
3.811	640	23.32	23.32	6
3.672	221	24.22	24.22	5
3.610	730	24.64	24.65	28
3.520	650	25.28	25.29	19
3.435	800	25.92	25.91	28
3.409	740	26.12	26.12	32
3.333	820/421	26.72	26.73/26.73	41
3.238	660	27.52	27.52	52
3.217	830/431	27.71	27.71/27.72	55
3.194	750/511	27.91	27.90/27.91	8
3.131	521	28.48	28.48	4
3.071	840/441	29.05	29.04/29.04	7
3.033	910	29.42	29.41	22
2.980	760	29.96	29.95	36
2.914	850	30.66	30.66	25
2.790	940/701	32.05	32.05/32.05	8
2.778	770	32.20	32.22	10
2.748	10,0,0/860	32.56	32.55/32.56	10
2.735	10,1,0/721	32.72	32.72/32.72	7
2.669	950/731	33.55	33.54/33.55	9
2.632	10,3,0/651	34.03	34.04/34.03	6
2.597	801	34.51	34.51	9
2.585	870/741	34.67	34.67/34.67	9
2.552	10,4,0/821	35.14	35.14/35.14	15
2.510	661	35.74	35.76	9
2.500	11,0,0/831	35.89	35.91/35.92	9
2.4886	11,1,0/751	36.06	36.07/36.07	5
2.4199	901	37.12	37.13	3
2.4087	970/911	37.30	37.27/37.28	6
2.3822	761	37.73	37.72	7
2.3474	11,4,0/851	38.31	38.30/38.31	10
2.2822	980/941	39.45	39.45/39.45	6
2.2586	12,2,0/10,0,1	39.88	39.87/39.88	6
2.1726	12,4,0	41.53	41.53	6
2.1661	871	41.66	41.67	3
2.1592	990	41.80	41.80	3
2.1077	11,7,0/11,1,1	42.87	42.87/42.87	4
2.0887	13,2,0/10,5,1	43.28	43.26/43.27	4
1.9836	12,0,1/002	45.70	45.71/45.72	26
1.9628	14,0,0/12,2,1/202	46.21	46.20/46.21/46.22	4
1.9434	10,10,0/222	46.70	46.70/46.72	5
1.9383	12,3,1/302	46.83	46.83/46.84	4
1.9328	312	46.97	46.96	5
1.9194	11,6,1/322	47.32	47.32/47.33	9
1.9053	12,8,0/12,4,1/402	47.69	47.68/47.69/47.70	7
1.9005	412	47.82	47.82	5
1.8867	14,4,0/10,8,1/422	48.19	48.17/48.17/48.18	13
1.8482	11,10,0/13,2,1/522	49.26	49.25/49.25/49.26	14
1.8267	532	49.88	49.85	7
1.8030	622	50.58	50.56	7
1.7997	13,8,0/11,8,1/542	50.68	50.66/50.66/50.67	10
1.7666	11,11,0/13,5,1/552	51.70	51.70/51.70/51.71	5
1.7375	13,9,0/11,9,1/732	52.63	52.61/52.61/52.62	9
1.7140	742	53.41	53.41	4
1.7039	14,8,0/14,4,1/822	53.75	53.73/53.74/53.75	10
1.6911	662	54.19	54.19	6
1.6874	12,11,0/832	54.32	54.29/54.30	8
1.6752	13,10,0/11,10,1	54.75	54.73/54.74	6
1.6659	14,4,0/842	55.08	55.06/55.08	3
1.6631	12,9,1/902	55.18	55.18/55.19	3
1.6601	15,7,0/15,1,1/912	55.29	55.28/55.29/55.30	7
1.6510	14,9,0/15,2,1/762	55.62	55.61/55.62/55.62	4
1.6393	16,5,0/13,8,1/852	56.05	56.04/56.05/56.06	11
1.6130	772	57.05	57.03	4
1.6090	16,6,0/12,10,1/862	57.20	57.23/57.23/57.24	4
1.5915	17,3,0/13,9,1/952	57.89	57.87/57.87/57.88	5

^{a/} This powder diffraction was obtained from material heated in a sealed Pt tube at 1280°C for 40 hours and quenched into water.

^{b/} This diffraction pattern was indexed with the aid of single crystal precession patterns on the basis of a tetragonal unit cell with $a = 7.484 \pm 0.003 \text{ \AA}$ and $c = 3.9656 \pm 0.0004 \text{ \AA}$.

tables 2–6 are given relative to the strongest peak height above background. The phases were found to have the structures (in order of increasing alkali content) of the Gatehouse tetragonal bronze-type (GTB), an orthorhombic distortion of the hexagonal tungsten bronze-type (HTB), and three hexagonal phases with c axes approximately $3.9 \text{ \AA} \times 9$, $\times 16$, and $\times 11$ which were called "9-layer", "16-layer", and "11-layer" phases in the $\text{K}_2\text{O}-\text{Ta}_2\text{O}_5$ system [1, 7].

Table 3

X-ray Diffraction Pattern of the Hexagonal Bronze-Like Phase From the Composition $21.75\text{Rb}_2\text{O} \cdot 78.25\text{Nb}_2\text{O}_5$.^{a/}

d_{obs}	hkl	$2\theta_{\text{obs}}$	$2\theta_{\text{calc}}$	I_{obs}
6.53	110	13.55	13.55	16
3.900	001	22.78	22.80	25
3.348	111	26.60	26.61	61
3.262	220	27.32	27.30	100
3.251	400	27.41	27.44	85
2.706	311	33.07	33.09	44
2.501	221	35.85	35.86	15
2.4966	401	35.94	35.96	15
2.0868	131	43.32	43.32	6
2.0810	421	43.45	43.44	8
1.9494	002	46.55	46.56	67
1.8998	331	47.84	47.84	14
1.8926	601	48.03	48.03	12
1.8880	040	48.16	48.17	21
1.8784	620	48.42	48.42	40
1.8077	530	50.44	50.44	2
1.6990	041	53.92	53.93	5
1.6923	621	54.15	54.16	11
1.6737	222	54.80	54.82	22
1.6709	402	54.90	54.89	17
1.6434	241	55.90	55.90	5
1.6396	331	56.04	56.03	6
1.6359	711	56.18	56.18	8
1.6319	440	56.33	56.33	17
1.6239	800	56.63	56.63	8
1.5054	441	61.55	61.56	5
1.4999	150	61.80	61.80	4
1.4002	151	66.75	66.77	4
1.3941	731/821	67.08	67.04/67.13	4
1.3556	042	69.25	69.24	6
1.3525	622	69.43	69.44	13
1.3396	351	70.20	70.23	3
1.3371	641	70.35	70.38	4
1.3325	911	70.63	70.64	4
1.3277	242	70.92	70.95	2
1.2994	003/10,0,0	72.71	72.72/72.73	3
1.2743	113	74.38	74.38	2
1.2508	442	76.02	76.00	4
1.2476	802	76.25	76.26	3
1.2313	840	77.45	77.47	2
1.2283	023/10,2,0	77.67	77.66/77.66	4

^{a/} This powder diffraction pattern was obtained from ground single crystal pulled from a melt of $21.75\text{Rb}_2\text{O} \cdot 78.25\text{Nb}_2\text{O}_5$ by the Czochralski method.

^{b/} This diffraction pattern was indexed with the aid of single crystal precession patterns on the basis of an orthorhombic unit cell with $a = 12.991 \pm 0.004 \text{ \AA}$, $b = 7.550 \pm 0.001 \text{ \AA}$ and $c = 3.8978 \pm 0.0008 \text{ \AA}$.

2.2. The System $\text{Rb}_2\text{O}-\text{Ta}_2\text{O}_5$

The system $\text{Rb}_2\text{O}-\text{Ta}_2\text{O}_5$ was investigated from 73.33 to 100 mol per cent Ta_2O_5 . Eight compositions were prepared by dry mixing Rb_2CO_3 and Ta_2O_5 , and heating at 500°C for 120 hours and 600°C for 110 hours with intermediate grindings. Portions from each composition were heated at higher temperatures in sealed Pt capsules in resistance wound quench-type furnaces and quenched into water.

Table 4

X-ray Diffraction Powder Pattern of the "9-L" Phase
Occurring at the Composition $\text{Rb}_2\text{O}:\text{Kb}_2\text{O}_5$ ^{a/}

d _{obs}	hkl	2θ _{obs}	2θ _{calc} ^{b/}	I _{obs}
18.16	002	4.86	4.86	3
9.11	004	9.70	9.72	100
6.515	100	13.58	13.59	25
6.058	006	14.61	14.61	15
5.378	103	15.43	15.44	6
4.852	105	18.27	18.28	4
4.564	008	19.51	19.52	40
3.728	108	23.85	23.86	7
3.473	114	25.63	25.62	34
3.433	109	25.93	25.94	90
3.252	200	27.40	27.37	34
3.245	201	27.46	27.49	36
3.195	116	27.90	27.91	29
3.174	1,0,10	28.09	28.09	8
3.142	203	28.38	28.37	49
3.064	204	29.12	29.11	13
3.027	0,0,12	29.48	29.46	68
2.969	205	30.07	30.05	44
2.896	118	30.85	30.85	38
2.868	206	31.16	31.16	4
2.758	207	32.44	32.43	7
2.732	1,0,12	32.57	32.57	14
2.646	208	33.85	33.88	14
2.613	1,1,10	34.29	34.29	7
2.597	0,0,14	34.51	34.51	7
2.535	209	35.38	35.38	16
2.4602	210	36.49	36.48	3
2.4557	211	36.56	36.57	4
2.4124	1,0,14/213	37.24	37.25/37.25	5
2.3581	1,1,12	38.13	38.12	10
2.2181	2,0,12	40.64	40.65	3
2.1696	2,0,13	42.59	42.59	6
2.1110	304	42.80	42.80	12
2.1026	219	42.98	43.00	11
2.0800	305	43.47	43.48	6
2.0429	306	44.30	44.30	10
2.0321	1,0,17	44.55	44.56	8
2.0200	0,0,18	44.83	44.84	65
1.9580	308	46.33	46.32	17
1.9438	2,0,15	46.69	46.69	12
1.9102	2,1,12	47.56	47.57	9
1.8790	220	48.40	48.39	41
1.8631	3,0,10/2,0,16	48.84	48.83/48.84	5
1.8409	224	49.47	49.48	5
1.8356	1,0,19	49.62	49.62	4
1.8054	310	50.51	50.50	4
1.7872	2,0,17	51.06	51.06	20
1.7667	3,0,12	51.76	51.78	5
1.7164	2,0,18	53.33	53.34	18
1.6726	1,0,21	54.83	54.83	6
1.6524	0,0,22	55.57	55.57	6
1.6488	2,0,23	55.70	55.71	12
1.6364	1,1,20	56.16	56.16	4
1.6271	400	56.51	56.49	5
1.6135	403	57.03	57.04	12
1.6019	404/1,0,22	57.48	57.47/57.49	5
1.5971	2,2,12	57.67	57.67	12
1.5888	405	58.00	58.02	5
1.5693	3,0,16	58.79	58.79	5
1.5513	3,1,12	59.54	59.55	5
1.5329	408	60.33	60.36	5
1.5281	2,0,21	60.54	60.53	24
1.5226	2,2,14	60.78	60.79	11
1.5149	0,0,24	61.12	61.13	4
1.5098	409	61.35	61.36	7
1.4934	320	62.10	62.09	2
1.4826	3,1,14/323	62.60	62.61/62.61	4
1.4786	3,0,18	62.79	62.80	5
1.4627	325	63.55	63.54	2
1.4538	4,0,12	64.99	64.99	2
1.4215	2,0,23	65.62	65.61	7
1.4187	328	65.77	65.76	5
1.4038	414	66.56	66.56	5
1.4004	329	66.74	66.71	8
1.3980	0,0,26	66.87	66.86	11
1.3793	3,1,17	67.90	67.88	4
1.3759	2,2,18	68.09	68.09	17
1.3557	418	69.25	69.23	5
1.3188	1,0,27	71.48	71.50	5
1.3024	500	72.52	72.54	3
1.2950	3,2,14/503	73.00	73.02/73.03	7
1.2674	4,0,18	74.86	74.86	7
1.2411	334/2,2,22	76.73	76.72/76.74	3
1.2299	421	77.56	77.57	2
1.2243	423	77.98	77.99	6
1.2158	2,1,26	78.63	78.64	2
1.2131	425	78.84	78.83	5
1.1858	4,0,21	81.02	81.02	6
1.1696	510	82.39	82.41	3
1.1530	4,2,11	83.84	83.83	5
1.1353	2,0,30	85.45	85.42	3
1.1216	2,2,26	86.75	86.73	7
1.0894	600	90.47	90.46	5
1.0792	3,1,27	91.09	91.06	2
1.0662	514/433	92.52	92.52/92.52	3
1.0582	3,0,40	93.43	93.45	2
1.0505	4,2,18	94.32	94.29	3

^{a/} This powder diffraction pattern was obtained from material heated in a sealed Pt tube at 1200°C for 88 hours and quenched into water.

^{b/} This diffraction pattern was indexed on the basis of a hexagonal unit cell with $a=7.5179\pm 0.0002\text{Å}$ and $c=36.353\pm 0.001\text{Å}$ by comparison with single crystal patterns of an apparently isostructural phase in the $\text{K}_2\text{O}:\text{Ta}_2\text{O}_5$ system.

Table 5

X-ray Diffraction Powder Pattern of the "16-L" Phase
Occurring at the Composition $25.58\text{Rb}_2\text{O}:74.58\text{K}_2\text{O}_5$ ^{a/}

d _{obs}	hkl	2θ _{obs}	2θ _{calc} ^{b/}	I _{obs}
16.35	004	5.40	5.42	5
10.89	006	8.11	8.14	14
8.16	008	10.83	10.86	23
6.51	0,0,10/100	14.59	14.59/13.60	33
6.49	101	14.64	14.66	40
6.24	103	16.19	16.20	5
6.05	104	16.63	16.65	5
5.82	105	15.21	15.21	7
5.58	106	15.86	15.87	11
4.655	0,0,14	19.06	19.07	21
4.377	1,0,11	20.27	20.26	7
3.757	110	23.66	23.66	7
3.661	114	24.29	24.29	6
3.550	116	25.06	25.06	15
3.449	1,0,16	25.81	25.80	79
3.413	118	26.09	26.10	39
3.301	1,0,17	26.99	26.99	20
3.250	1,1,10/200	27.42	27.49/27.39	100
3.191	204	27.94	27.94	21
3.156	205	28.25	28.25	15
3.115	206	28.63	28.62	54
3.070	207	29.06	29.05	20
3.020	208	29.55	29.54	43
2.968	209	30.08	30.09	50
2.960	0,0,22	30.17	30.17	48
2.922	1,1,14	30.57	30.56	43
2.796	1,0,21	31.98	31.95	14
2.761	1,1,16	32.40	32.41	5
2.712	0,0,24	33.00	32.99	7
2.693	1,0,22	33.24	33.23	7
2.683	1,1,17	33.37	33.38	4
2.667	2,0,14	33.57	33.59	7
2.603	0,0,25/2,0,15	34.42	34.40/34.42	13
2.540	2,0,16	35.31	35.29	21
2.503	0,0,26/1,0,24	35.85	35.83	6
2.4595	210	36.50	36.50	6
2.1111	307	42.80	42.77	9
2.1055	2,1,16	42.92	42.93	10
2.0957	308	43.13	43.13	12
2.0788	309	43.50	43.52	8
2.0581	3,0,10	43.96	43.96	20
2.0342	2,1,18	44.50	44.51	39
1.9766	1,1,28	45.87	45.85	6
1.9658	3,0,14	46.14	46.14	10
1.9267	1,1,29/2,1,21	47.13	47.11/47.13	6
1.8779	220/221	48.43	48.42/48.44	48
1.8304	228	49.78	49.78	4
1.8048	2,0,30/3,0,20 2,2,10/310	50.53 50.53/50.53	50.51/50.52 50.53/50.53	18
1.7876	2,1,25/315	51.05	51.03/51.05	19
1.7645	2,0,31	51.76	51.76	9
1.7599	0,0,37	51.91	51.91	8
1.7496	3,0,22	52.24	52.24	8
1.6943	3,0,24	54.08	54.09	5
1.6868	2,0,33/2,2,17	54.34	54.33/54.35	6
1.6587	2,1,29	55.34	55.36	4
1.6570	1,0,38	55.40	55.40	11
1.6500	3,1,16	55.66	55.67	4
1.6329	3,1,17	56.29	56.30	4
1.6279	0,0,40	56.48	56.48	8
1.6261	401	56.55	56.54	10
1.6222	403	56.70	56.70	6
1.6122	3,0,27	57.08	57.06	4
1.6092	406	57.20	57.21	11
1.5956	408	57.73	57.75	15
1.5863	3,0,28/2,2,22	58.10	58.11/58.11	10
1.5594	1,1,38	59.20	59.22	4
1.5480	2,0,37	59.68	59.69	4
1.5442	2,2,24	59.84	59.84	7
1.5356	4,0,14	60.21	60.22	4
1.5233	2,2,25/4,0,15	60.75	60.74/60.75	10
1.5149	0,0,43	61.12	61.15	15
1.5109	2,1,34/4,0,16	61.30	61.30/61.32	12
1.5027	2,2,26/3,1,24	61.67	61.67/61.68	9
1.4927	320/321	62.13	62.13/62.15	7
1.4888	323	62.31	62.29	6
1.4794	0,0,44/326	62.75	62.73/62.78	6
1.4217	3,2,14	65.61	65.63	4
1.4152	0,0,46	65.95	65.94	14
1.4078	416	66.34	66.34	5
1.4044	1,1,43	66.52	66.52	5
1.4009	3,2,16	66.71	66.68	10
1.3801	2,2,32/3,2,18	67.85	67.85/67.86	12
1.3760	1,1,44	68.08	68.03	11
1.3171	4,0,29	71.58	71.57	5
1.3012	500/501	72.59	72.58/72.60	14

^{a/} This powder diffraction pattern was obtained from material heated in a sealed Pt tube at 1275°C for 117 hours and quenched into water.

^{b/} This pattern was indexed on the basis of a hexagonal unit cell with $a=7.5138\pm 0.0005\text{Å}$ and $c=65.115\pm 0.009\text{Å}$.

Table 6

X-ray Diffraction Pattern of the "11-L" Phase Occurring at the Composition $4\text{Rb}_2\text{O}:11\text{Nb}_2\text{O}_5$.^{a/}

d_{obs}	hkl	$2\theta_{\text{obs}}$	$2\theta_{\text{calc}}$	I_{obs}
14.41	003	6.13	6.14	8
7.19	006	12.30	12.29	23
6.44	101	13.74	13.74	21
6.23	012	14.17	14.19	4
5.58	104	15.86	15.88	9
4.792	009	18.50	18.48	6
4.160	018	21.34	21.36	4
3.759	110	23.65	23.64	2
3.639	113	24.44	24.44	9
3.599	1,0,10/0,0,12	24.72	24.72/24.72	10
3.361	0,1,11	26.48	26.49	61
3.334	116	26.72	26.72	71
3.247	021	27.45	27.44	22
3.212	202	27.65	27.67	6
3.117	024	28.62	28.60	19
3.049	205	29.27	29.28	100
2.958	1,0,13	30.19	30.18	16
2.877	0,0,15	31.06	31.04	68
2.789	208	32.07	32.07	8
2.601	0,2,10/1,1,12	34.45	34.46/34.47	22
2.4921	1,0,16	36.01	35.99	5
2.3983	0,0,18	37.47	37.46	3
2.2851	1,1,15	39.40	39.38	5
2.1461	1,0,19	42.07	42.07	4
2.0855	1,2,11	43.35	43.34	12
2.0797	306	43.48	43.50	20
2.0554	0,0,21	44.02	44.00	71
2.0227	1,1,18	44.77	44.77	5
2.0024	2,0,17	45.25	45.23	7
1.9788	309	45.82	45.83	8
1.9240	1,2,14	47.20	47.19	4
1.8817	220	48.33	48.36	52
1.8653	223	48.78	48.80	4
1.8189	226	50.11	50.09	12
1.8034	1,1,21/0,1,23	50.57	50.55/50.55	10
1.7998	2,0,20/0,0,24	50.68	50.69/50.70	18
1.7685	315/1,2,17	51.64	51.64/51.66	2
1.7508	229	52.20	52.20	1
1.6692	1,0,25	54.96	54.95	2
1.6662	1,3,10/2,2,12	55.07	55.05	2
1.6416	3,1,11	55.97	55.98	27
1.6273	401	56.50	56.50	1
1.6234	1,2,20/1,1,24	56.65	56.66/56.67	2
1.6096	0,1,26	57.18	57.20	3
1.6010	045	57.52	57.54	12
1.5989	0,0,27	57.60	57.59	7
1.5873	1,3,13	58.06	58.07	1
1.5745	407/2,2,15	58.58	58.57/58.58	18
1.5594	048/3,1,14	59.20	59.21/59.22	3
1.5343	2,1,22	60.27	60.25	2
1.5249	0,2,25/4,0,10	60.68	60.64/60.73	14
1.5011	1,0,28	61.75	61.77	4
1.4935	321	62.10	62.09	6
1.4793	2,0,26	62.76	62.75	8
1.4387	0,0,30	64.74	64.71	12
1.4142	1,3,19/2,1,25	66.00	66.00/66.01	1
1.3943	416/4,0,16	67.07	67.05/67.07	8
1.3873	2,2,21	67.45	67.43	8
1.3627	419/3,2,13	68.84	68.82/68.83	3
1.3076	3,2,16	72.18	72.20	5
1.2995	0,4,20/2,2,24	72.70	72.66/72.67	12
1.2737	1,2,29	74.42	74.40	1

^{a/} This powder diffraction pattern was obtained from material heated in a sealed Pt tube at 1306°C for 22 hours and quenched into water.

^{b/} This diffraction pattern was indexed with the aid of single crystal precession patterns on the basis of a hexagonal unit cell with $a=7.5224\pm0.0007\text{\AA}$ and $c=43.180\pm0.005\text{\AA}$, $h+k+l=3n$.

pyrometer recalibrated against the melting points of palladium and platinum 1554 and 1772 °C [6]. The pyrometer uncertainty is estimated at $\pm 10^\circ$ to 1700 °C and $\pm 15^\circ$ at 1750 °C. The variation in structure type with alkali content was similar to that observed in the $\text{Rb}_2\text{O}-\text{Nb}_2\text{O}_5$ system with the exception of the low temperature unindexed phase. Samples were identified at room temperature by x-ray powder diffraction using Ni-filtered Cu radiation and a $1/4^\circ$ $2\theta/\text{min}$ scanning rate. The x-ray diffraction powder patterns derived from quenched specimens were used to construct the phase diagram shown in figure 2 and the experimental results are listed in table 7. X-ray diffraction patterns for all the phases in this subsystem are given in tables 8–11. Intensities listed in tables 8–11 are given relative to the strongest peak height above background.

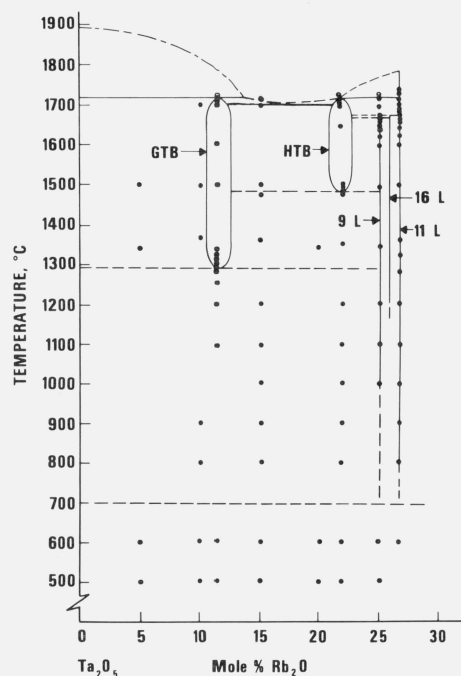


FIGURE 2. Phase diagram for the system $\text{Ta}_2\text{O}_5:4\text{Rb}_2\text{O}:11\text{Ta}_2\text{O}_5$.

2.3. Crystal Growth

Many of the phases discovered during the phase equilibria studies of the alkali niobate and tantalate systems have not been previously reported in the literature. One of the objectives of the crystal growth portion of this study has been to synthesize single crystals for x-ray diffraction studies to provide crystallographic information on these materials to assist in the interpretation of x-ray diffraction powder patterns. The second, and equally important objective, has been to grow large single crystals of potentially useful Rb^+ phases for use in studies of ion exchange behavior for the purpose of obtaining Na^+ and/or K^+ analogues.

Temperature was measured with a 100 Pt/90 Pt-10 Rh thermocouple calibrated against the melting points of gold and palladium. The temperatures reported are considered to be accurate to $\pm 5^\circ\text{C}$ up to 1500 °C. Above 1550 °C temperatures were measured with a NBS calibrated optical

Table 7. Experimental Data for the System Ta_2O_5 - $4Rb_2O$: $11Ta_2O_5$.

Composition	Initial Heat Treatment		Final Heat ^{a/} Treatment		Results of Physical Observation	Results of X-ray Diffraction Analysis
	Temp. °C	Time hr	Temp. °C	Time hr		
$5Rb_2O$: $95Ta_2O_5$	500	120	500	120 ^{b/}		L-Ta ₂ O ₅
	500	120	600	110 ^{b/}		
	600	110				
			1340	120		L-Ta ₂ O ₅ + GTB
			1500	144		H-Ta ₂ O ₅ + GTB
$10Rb_2O$: $90Ta_2O_5$	500	120	500	120 ^{b/}		--
	500	120	600	110 ^{b/}		L-Ta ₂ O ₅
	600	90				
			800	80		L-Ta ₂ O ₅ + 9L
			900	60		L-Ta ₂ O ₅ + 9L
			1366	120		GTB + L-Ta ₂ O ₅
			1500	120		GTB + H-Ta ₂ O ₅ (tr)
			1700	1		GTB
$11.5Rb_2O$: $88.5Ta_2O_5$	500	120	500	120 ^{b/}		--
	500	120	600	110 ^{b/}		--
	600	110				
			1098	136		L-Ta ₂ O ₅ + 9L
			1255	27		9L + L-Ta ₂ O ₅
			1318	16		9L + L-Ta ₂ O ₅
			1340	120		GTB
			1500	144		GTB
			1603	24		GTB
	1200	150				
			1296	91		L-Ta ₂ O ₅ + 9L + GTB (tr)
			1297	117		GTB + L-Ta ₂ O ₅
			1307	64		GTB + L-Ta ₂ O ₅
			1317	67		GTB + L-Ta ₂ O ₅
			1327	18		GTB + L-Ta ₂ O ₅
			1330	115		GTB + L-Ta ₂ O ₅
			1332	16		GTB + L-Ta ₂ O ₅
			1340	72		GTB
			1704	0.5	not melted	
			1709	0.5	not melted	
			1714	.25	not melted	
			1721	2	partially melted	GTB
			1722	1	completely melted	
	1330	115				
			1317	67		GTB
	1340	72				
			1277	136		GTB
			1297	117		GTB
	1277	136				
			1331	115		GTB
$15Rb_2O$: $85Ta_2O_5$	500	120	500	120 ^{b/}		
	500	120	600	110 ^{b/}		
	600	110				
			800	80		L-Ta ₂ O ₅ + 9L
			900	60		L-Ta ₂ O ₅ + 9L
			1000	40		L-Ta ₂ O ₅ + 9L
			1098	136		L-Ta ₂ O ₅ + 9L
			1360	120		GTB + 9L
			1473	65		GTB + 9L
			1500	17.5		GTB + HTB
			1500	18		GTB + HTB
			1500	144		GTB + HTB
			1700	2		GTB + HTB
	1200	150				
			1707	0.5	not melted	
			1711	0.5	not melted	
			1714	0.5	completely melted	
			1715	0.5	completely melted	
$20Rb_2O$: $80Ta_2O_5$	500	120	500	120 ^{b/}		
	500	120	600	110 ^{b/}		
	600	110				
			1340	120		9L + GTB

In general, the choice of technique was dictated by the characteristics of the desired phase, i.e., congruent or incongruent melting, volatility of one or more of the components, range of coexistence with liquid, and the desired final size of the crystal. Both fluxed melt and Czochralski techniques were utilized, and in some cases, the flux evaporation technique was used for the preparation of small crystals.

2.4. Czochralski Crystal Growth

a. $4Rb_2O$: $11Nb_2O_5$

A 100 gram batch of $29Rb_2O$: $71Nb_2O_5$ was calcined at 400 °C for 60 hours for use as a starting material. Five boules were pulled and the remaining charge discarded. The five boules were remelted and used as a "purified" charge

Table 7. Experimental Data for the System $Ta_2O_5-4Rb_2O:11Ta_2O_5$. (cont.)

21.75Rb ₂ O:78.25Ta ₂ O ₅	500	120	500	120 ^{b/}		
	500	120	600	110 ^{b/}		
	600	110				
			800	80		9L + L-Ta ₂ O ₅
			900	60		9L + L-Ta ₂ O ₅
			1000	40		9L + L-Ta ₂ O ₅
			1100	138		9L + L-Ta ₂ O ₅
			1360	120		9L + L-Ta ₂ O ₅
			1473	65		9L + GTB
			1500	18		9L + GTB
			1643	24		HTB + 9L (tr)
			1700	2		HTB
			1700	1		HTB
			1706	1		HTB
	1200	150	1474	67		9L + GTB
			1477	23		9L + GTB
			1477	18		9L + GTB
			1479	17		9L + GTB
			1479	18		9L + GTB
			1480	17		9L + GTB
			1482	18		9L + HTB (?)
			1482	45		9L + GTB
			1484	20		9L + GTB
			1486	41		9L + GTB
			1488	16		9L + HTB
			1488	16		9L + HTB
			1498	21		9L + HTB
			1706	1	not melted	
			1716	1	not melted	HTB
			1717	0.5	partially melted	
			1721	2	partially melted	HTB
25Rb ₂ O:75Ta ₂ O ₅	500	120	500	120 ^{b/}		L-Ta ₂ O ₅
	500	120	600	110 ^{b/}		
	600	110				
			1000	40		9L + L-Ta ₂ O ₅ (tr)
			1100	138		9L
			1344	120		9L
			1498	144		9L + ? (tr)
			1675	18		16L + HTB
			1700	1		16L + HTB
			1700	1		16L + HTB
			1715	1	not melted	
	1200	150	1600	20		9L
			1621	3		9L
			1624	17		9L
			1641	21		9L
			1659	19		9L
			1663	67		9L + HTB (tr)
			1677	29		9L + HTB + 16L
			1682	18		16L + HTB
			1722	16	partially melted	
			1725	16	partially melted	16L + HTB
26.7Rb ₂ O:73.3Ta ₂ O ₅	500	120	500	120 ^{b/}		L-Ta ₂ O ₅ + 2:3
	500	120	600	110 ^{b/}		
	600	110				
			800	80		11L + 2:3
			900	60		11L + 2:3
			1000	40		11L + 2:3
			1098	136		11L + 2:3
			1360	120		16L + 11L
			1500	120		16L + 11L
			1596	24		16L + 11L
			1625	16		16L + 11L
			1640	2		16L + 11L
			1647	1		16L + 11L
			1700	1		11L
			1710	1	not melted	
	1200	150	1283	72		16L + 11L
			1672	1		11L
			1719	1	not melted	
			1725	0.5		11L
			1726	16		11L

^{a/} Except as indicated by ^{b/} the samples were quenched into water from the temperature indicated.

^{b/} The samples were heated at the temperatures indicated in open Pt crucibles. Due to the volatility of Rb₂O the bulk composition may have shifted to one higher in mole percent Ta₂O₅.

Table 8

X-ray Diffraction Pattern of $11.5\text{Rb}_2\text{O}:88.5\text{Ta}_2\text{O}_5$,^{a/}

d_{obs}	hkl	$2\theta_{\text{obs}}$	$2\theta_{\text{calc}}$	I_{obs}
19.66	110	4.49	4.53	5
13.84	200	6.38	6.41	5
12.39	210	7.13	7.16	6
9.77	220	9.04	9.06	8
8.73	310	10.12	10.14	6
7.67	320	11.53	11.56	10
6.70	410	13.20	13.23	8
5.12	520	17.31	17.31	3
4.873	440	18.19	18.19	3
4.731	530	18.74	18.75	3
3.902	001	22.77	22.77	100
3.826	111	23.23	23.23	10
3.754	201	23.68	23.68	3
3.622	730	24.56	24.57	23
3.560	311	24.99	24.98	6
3.531	650	25.20	25.21	10
3.475	321	25.61	25.61	8
3.446	800	25.83	25.83	19
3.422	740	26.02	26.03	25
3.370	411	26.43	26.46	10
3.369	331	26.63	26.63	33
3.250	660	27.42	27.43	41
3.227	830	27.62	27.62	39
3.163	511	28.19	28.18	3
3.045	910	29.30	29.31	19
2.992	760	29.84	29.85	29
2.958	611	30.19	30.20	3
2.924	850	30.55	30.56	26
2.800	940	31.93	31.94	10
2.757	860	32.45	32.45	12
2.731	641	32.76	32.77	5
2.718	721	32.93	32.93	5
2.653	731	33.75	33.75	13
2.617	651	34.22	34.23	7
2.584	801	34.69	34.70	10
2.572	741	34.86	34.86	12
2.540	821	35.31	35.32	17
2.4966	661	35.94	35.94	13
2.4873	831	36.08	36.09	12
2.4006	911	37.43	37.43	9
2.3737	761	37.87	37.87	14
2.3392	851	38.45	38.45	15
2.2744	941	39.59	39.59	6
2.2510	861	40.02	40.01	6
2.1796	12,4,0	41.39	41.39	6
2.1666	990	41.65	41.66	3
2.1152	11,7,0	42.71	42.72	3
2.1091	11,0,1	42.84	42.85	3
1.9497	10,10,0	46.54	46.54	27
1.9259	13,6,0	47.15	47.16	8
1.9027	12,4,1	47.76	47.76	5
1.8934	14,4,0	48.01	48.00	14
1.8542	11,10,0	49.09	49.08	13
1.8339	15,1,0	49.67	49.67	6
1.8060	13,8,0	50.49	50.48	14
1.7723	11,11,0	51.52	51.52	4
1.7437	10,10,1/15,5,0	52.43	52.42/52.43	10
1.7266	13,6,1	52.99	52.98	3
1.7229	16,0,0	53.11	53.10	3
1.7173	732	53.30	53.30	3
1.7066	15,6,0	53.66	53.66	5
1.7031	14,4,1	53.78	53.76	8
1.6984	802	53.94	53.96	6
1.6934	12,11,0	54.11	54.10	8
1.6842	13,7,1	54.43	54.43	6
1.6746	11,10,1	54.77	54.75	9
1.6715	16,4,0	54.88	54.87	13
1.6692	832	54.96	54.95	12
1.6595	15,1,1	55.31	55.30	8
1.6412	14,6,1	55.98	55.95	8
1.6388	13,8,1	56.07	56.06	13
1.6216	15,8,0	56.72	56.71	5
1.6189	13,11,0	56.82	56.82	5
1.6140	11,11,1/16,6,0	57.01	57.02	7
1.6086	12,10,1	57.22	57.24	2
1.5918	15,5,1	57.88	57.87	7
1.5784	16,7,0	58.42	58.40	10
1.5664	14,8,1	58.92	58.92	3
1.5534	12,11,1	59.45	59.44	4
1.5482	14,11,0	59.67	59.66	4
1.5366	16,4,1	60.17	60.18	4
1.4997	12,12,1/17,7,0	61.81	61.80/61.81	3
1.4979	15,8,1	61.89	61.90	3
1.4952	14,12,0	62.02	62.00	7
1.4627	16,7,1	63.55	63.52	7
1.4611	16,10,0	63.63	63.62	6
1.4389	14,11,1	64.73	64.71	4
1.4336	11,7,2/16,8,1/ 19,3,0	65.00	64.99/65.00/ 65.01	2
1.3996	18,8,0	66.78	66.77	3
1.3844	14,1,2	67.61	67.62	3
1.3688	16,10,1	68.49	68.51	4
1.3583	19,1,1	69.09	69.09	5
1.3534	19,2,1	69.38	69.37	4
1.3435	15,14,0	69.97	69.95	3
1.3404	18,7,1	70.15	70.13	4
1.3359	15,1,2	70.42	70.40	4
1.3248	17,12,0	71.10	71.09	4
1.3155	16,12,1/15,15,0	72.68	72.68/72.69	5

Table 9

X-ray Diffraction Powder Pattern of $21.75\text{Rb}_2\text{O}:78.25\text{Ta}_2\text{O}_5$,^{a/}

d_{obs}	hkl	$2\theta_{\text{obs}}$	$2\theta_{\text{calc}}$	I_{obs}
6.52	100	13.56	13.57	31
3.907	001	22.74	22.74	29
3.768	110	23.59	23.61	3
3.35	101	26.57	26.57	38
3.26	200	27.34	27.33	100
2.71	111	33.02	33.01	41
2.50	201	35.85	35.84	52
2.4663	210	36.40	36.42	7
2.1752	300	41.48	41.51	4
2.0851	211	43.36	43.37	14
1.9542	002	46.43	46.44	21
1.8998	301	47.84	47.84	21
1.8824	220	48.31	48.30	40
1.8719	102	48.60	48.61	5
1.8088	310	50.41	50.41	6
1.6962	221	54.02	54.02	19
1.6761	202	54.72	54.73	26
1.6416	311	55.97	55.98	11
1.6304	400	56.39	56.39	18
1.5304	212	60.44	60.41	4
1.5046	401	61.59	61.59	18
1.4958	320	61.99	61.97	2
1.3973	321	66.91	66.91	9
1.3555	222	69.26	69.25	16
1.3370	411	70.36	70.35	5
1.3271	312	70.96	70.95	3
1.2769	103	74.21	74.19	2

a/ This powder diffraction pattern was obtained from material heated in a sealed Pt tube at 1706°C for 1 hour and quenched into water.

b/ This diffraction pattern was indexed with the aid of single crystal precession patterns on the basis of a hexagonal unit cell with $a=7.5306 \pm .0005 \text{ \AA}$ and $c=3.9072 \pm .0005 \text{ \AA}$.

for the actual crystal growth experiments. From this "purified" charge large, clear single crystal boules of the "11-layer" phase were grown. The "11-layer" crystals show a marked preference for growth perpendicular to the c axis and at least one excellent cleavage (basal-plane) is evident. Density measurements made with a double pan liquid displacement apparatus gave a value of $4.40 \pm .05 \text{ g/cm}^3$.

b. $21.75\text{Rb}_2\text{O}:78.25\text{Nb}_2\text{O}_5$ (HTB)

Crystals of the hexagonal tungsten bronze (HTB) phase in this system were grown by pulling from a melt of the composition $21.75\text{Rb}_2\text{O}:78.25\text{Nb}_2\text{O}_5$ (experiments performed at NBS by C. Jones as part of the American University Research Participation Program). Large, clear, water-white crystals were easily obtained but all fractured into large blocks during cooling. The fracture may be related to a non-quenchable symmetry change from a high temperature hexagonal form to the room temperature orthorhombic form, or to extreme anisotropy of thermal expansion.

c. $11.5\text{Rb}_2\text{O}:88.5\text{Nb}_2\text{O}_5$ (GTB)

Crystals of the Gatehouse tetragonal bronze (GTB) phase were grown from a composition of $16\text{Rb}_2\text{O}:84\text{Nb}_2\text{O}_5$ (experiments performed by D. Klein at NBS as part of the American University Research Participation Program). Small single crystal boules were successfully pulled from the melt, but again fractures developed during cooling.

a/ This powder diffraction pattern was obtained from material heated in a sealed Pt tube at 1340°C for 72 hours and quenched into water.

b/ This diffraction pattern was indexed with the aid of the single crystal pattern of the $11.5\text{K}_2\text{O}:88.5\text{Nb}_2\text{O}_5$ analogue on the basis of a tetragonal unit cell with $a=27.515 \pm .002 \text{ \AA}$ and $c=3.9018 \pm .0005 \text{ \AA}$.

Table 10

X-ray Diffraction Powder Pattern of the "9-1" Phase
Occurring at the Composition $\text{Rb}_2\text{O} \cdot 3\text{Ta}_2\text{O}_5$ ^{a/}

d_{obs}	hkl	$2\theta_{\text{obs}}$	$2\theta_{\text{calc}}^b/$	I_{obs}
9.13	004	9.68	9.71	19
8.51	100	13.59	13.61	70
8.40	101	13.82	13.80	9
6.08	006	14.56	14.59	6
5.74	103	15.43	15.45	14
4.855	105	18.26	18.28	9
4.558	008	19.46	19.49	12
3.729	108	23.84	23.85	7
3.678	112	24.18	24.19	3
3.472	114	25.64	25.65	45
3.431	109	25.95	25.92	80
3.252	200	27.40	27.41	46
3.237	201	27.53	27.52	63
3.194	116	27.91	27.93	35
3.137	203	28.43	28.40	100
3.061	204	29.15	29.14	33
3.033	0,0,12	29.43	29.42	29
2.968	205	30.08	30.08	65
2.896	118	30.85	30.85	47
2.867	206	31.17	31.19	12
2.759	207	32.42	32.45	6
2.752	119	32.51	32.51	12
2.748	1,0,12	32.56	32.54	12
2.646	208	33.85	33.86	27
2.601	0,0,14	34.45	34.46	9
2.534	209	35.40	35.39	50
2.4576	210	36.53	36.53	13
2.4531	211	36.60	36.62	10
2.4144	1,0,14	37.21	37.21	6
2.3588	1,1,12	38.12	38.11	5
2.3306	215	38.60	38.64	4
2.2176	2,0,12	40.65	40.64	4
2.1671	300	41.64	41.64	2
2.1626	301	41.73	41.72	2
2.1210	2,0,13	42.59	42.57	7
2.1097	304	42.83	42.86	12
2.1001	219	43.02	43.03	17
2.0779	305	43.52	43.53	2
2.0417	306	44.33	44.35	8
2.0364	2,1,10	44.45	44.44	8
2.0222	0,0,18	44.78	44.77	21
1.9562	308	46.38	46.37	17
1.9446	2,0,15	46.67	46.66	7
1.9096	2,1,12	47.58	47.58	9
1.8759	220	48.49	48.46	79
1.8635	2,0,16	48.83	48.81	3
1.8388	224/1,0,19	49.53	49.55/49.55	6
1.8031	310	50.58	50.57	7
1.7941	312/226	50.85	50.84/50.88	5
1.7875	2,0,17	51.05	51.03	27
1.7859	2,1,14	51.10	51.10	26
1.7843	313	51.15	51.17	21
1.7628	3,0,12	51.82	51.80	3
1.7352	228	52.71	52.71	5
1.7174	2,0,18	53.30	53.30	12
1.7150	3,0,13	53.38	53.41	13
1.6752	1,0,21	54.75	54.75	2
1.6678	2,2,10	55.01	55.00	2
1.6540	0,0,22	55.51	55.48	2
1.6467	319	55.78	55.77	16
1.6252	400	56.58	56.57	9
1.6239	401	56.63	56.64	8
1.6110	403	57.13	57.13	13
1.5999	404	57.56	57.55	10
1.5962	2,2,12	57.71	57.71	20
1.5864	405	58.10	58.10	11
1.5703	406	58.75	58.76	3
1.5410	3,1,12	59.60	59.59	5
1.5303	408	60.44	60.42	14
1.5287	2,0,21	60.51	60.47	21
1.5221	2,2,14	60.80	60.81	12
1.5080	409	61.43	61.42	15
1.4912	320	62.20	62.18	3
1.4816	3,1,14	62.65	62.64	5
1.4805	323	62.70	62.70	5
1.4778	1,0,24	62.83	62.85	2
1.4592	4,0,11	63.72	63.73	5
1.4223	2,0,23	65.58	65.54	3
1.4192	0,0,26	66.74	66.75	5
1.3989	329	66.82	66.79	11
1.3783	4,0,14	67.95	67.95	4
1.3753	2,2,18/2,0,24	68.12	68.09/68.16	18
1.3544	418	69.32	69.32	6
1.3382	3,2,12	70.28	70.26	3
1.3219	4,1,10	71.28	71.28	3
1.2940	3,2,14	73.06	73.07	8

^{a/} This powder diffraction pattern was obtained from material heated in a sealed Pt tube at 1659°C for 16 hours and quenched into water.^{b/} This diffraction pattern was indexed with the aid of single crystal precession patterns on the basis of a hexagonal unit cell with $a=7.5078 \pm .0006 \text{ \AA}$ and $c=36.408 \pm .005 \text{ \AA}$.

Table 11

X-ray Diffraction Powder Pattern of $4\text{Rb}_2\text{O} \cdot 11\text{Ta}_2\text{O}_5$ ^{a/}

d_{obs}	hkl	$2\theta_{\text{obs}}$	$2\theta_{\text{calc}}^b/$	I_{obs}
14.43	003	6.12	6.13	5
7.20	006	12.28	12.28	20
6.43	101	13.75	13.76	30
6.23	102	14.20	14.22	5
5.57	104	15.90	15.90	16
5.18	105	17.05	17.06	2
4.800	009	18.47	18.47	3
4.157	108	21.36	21.38	6
3.632	113	24.49	24.49	10
3.599	0,0,12/1,0,10	24.72	24.71/24.73	10
3.357	1,0,11	26.53	26.50	44
3.326	116	26.78	26.77	59
3.240	201	27.51	27.50	23
3.217	202	27.71	27.73	4
3.149	1,0,12	28.32	28.32	4
3.112	204	28.66	28.66	17
3.041	205	29.35	29.33	100
2.956	1,0,13	30.21	30.18	20
2.881	0,0,15	31.02	31.03	35
2.787	1,0,14	32.08	32.09	12
2.597	2,0,10	34.51	34.51	38
2.504	2,0,11	35.84	35.83	8
2.4941	1,0,16	35.98	35.99	8
2.4532	211	36.60	36.60	5
2.4013	0,0,18	37.42	37.45	4
2.3952	214	37.52	37.51	4
2.3237	2,0,13	38.72	38.72	2
2.2840	1,1,15	39.42	39.41	4
2.2512	1,0,18	40.02	40.02	1
2.2367	218	40.29	40.30	3
2.1461	1,0,19	42.07	42.07	4
2.1436	303	42.12	42.14	5
2.0829	2,1,11	43.41	43.41	11
2.0756	306	43.57	43.58	19
2.0567	0,0,21	43.99	43.99	17
2.0453	307	44.26	44.27	3
2.0201	1,1,18	44.83	44.79	3
2.0019	2,0,17	45.26	45.26	3
1.9747	309	45.92	45.91	7
1.9218	2,1,14	47.26	47.25	7
1.8762	220	48.48	48.47	38
1.8614	223	48.89	48.91	3
1.8162	226	50.19	50.20	12
1.8028	310	50.59	50.58	15
1.7988	2,0,20	50.71	50.71	29
1.7776	314	51.36	51.33	3
1.7660	2,1,17	51.72	51.71	3
1.7478	229	52.30	52.30	2
1.6682	2,2,12	55.00	54.98	2
1.6638	3,1,10	55.16	55.16	3
1.6377	3,1,11	56.11	56.08	8
1.6234	1,1,24	56.65	56.68	6
1.6092	1,0,26	57.20	57.18	6
1.5963	405	57.70	57.67	18
1.5712	407	58.71	58.70	27
1.5564	408	59.33	59.34	4
1.5331	2,1,22	60.32	60.29	2
1.5251	2,0,25	60.67	60.65	12
1.5208	4,0,10	60.86	60.85	15
1.4986	3,1,16	61.86	61.83	6
1.4903	321	62.24	62.24	7
1.4786	2,2,18	62.79	62.81	9
1.4393	0,0,30	64.71	64.69	5
1.4357	2,0,27	64.89	64.91	4
1.3932	0,0,31	67.13	67.12	6
1.3911	416	67.24	67.21	10
1.3859	2,2,21	67.53	67.51	9
1.3758	2,1,26	68.09	68.07	4
1.3608	419	68.95	68.98	3
1.3422	3,2,14	70.04	70.01	2
1.2980	502	72.80	72.82	8

^{a/} This powder diffraction pattern was obtained from material heated in a sealed Pt tube at 1719°C for 1 hour and quenched into water.^{b/} This diffraction pattern was indexed with the aid of single crystal precession patterns on the basis of a hexagonal unit cell with $a=7.5065 \pm .0007 \text{ \AA}$ and $c=43.194 \pm .005 \text{ \AA}$, $h+k+l=3n$.

2.5 Flux Evaporation Crystal Growth

a. The Systems $\text{Rb}_2\text{O-Nb}_2\text{O}_5$ and $\text{Rb}_2\text{O-Ta}_2\text{O}_5$ With MoO_3

Nine different compositions of two grams each were prepared from Rb_2CO_3 , Nb_2O_5 , and MoO_3 . These samples were placed in 5 mL Pt crucibles and heated to 900–1100 °C in an induction furnace. Small crystals (~2 mm) of the "11-layer" phase were obtained from compositions of 30:5:65 and 30:10:60 ($\text{Rb}_2\text{O:Nb}_2\text{O}_5:\text{MoO}_3$). A 27.5:10:62.5 composition yielded small crystals of the GTB phase plus $\text{H-Nb}_2\text{O}_5$ while a 28:6:67 composition yielded single crystals of the HTB phase. No crystals of the unidentified phase occurring at about 15 mol per cent Rb_2O were obtained by the flux evaporation technique.

Six different compositions in the $\text{Rb}_2\text{O-Ta}_2\text{O}_5\text{-MoO}_3$ system were prepared and heated as in the $\text{Rb}_2\text{O-Nb}_2\text{O}_5\text{-MoO}_3$ system. The 30:10:60 and 35:5:60 compositions when heated to 1100 °C yielded single crystals of the "9-layer" phase. No other compositions yielded crystals of phases found in the subsystem being studied.

b. The System $\text{Rb}_2\text{O-Ta}_2\text{O}_5\text{:RbF}$

In view of the success obtained by the flux evaporation synthesis route using KF in the $\text{KSbO}_3\text{-KF}$ system [8], similar attempts were made using RbF and Ta_2O_5 in an attempt to obtain rubidium tantalate crystals. However, RbTa_2O_5 with the pyrochlore structure was the only identified product. A 95RbF:5 Ta_2O_5 composition was completely liquid at 925 °C and on cooling yielded acicular crystals of an unknown phase. Clear, euhedral octahedra of the $\text{RbTa}_2\text{O}_5\text{F}$ pyrochlore were obtained from a composition of 75RbF:25 Ta_2O_5 heated to about 1150 °C for 30 seconds.

2.6. Ion Exchange

One of the best screening tests for the ionic conductivity of a solid phase is to determine whether or not the alkali ion in the structure can be exchanged with a different alkali ion. This may be tested by heating in a large excess of a molten salt (or solution) containing the second ion. A large number of experiments of this type were performed on many different compounds found in this study. In this paper, the terms "single ion exchange" and "double ion exchange" refer to the exchange of K^+ or Na^+ for Rb^+ and the sequential exchange of K^+ for Rb^+ followed by Na^+ for K^+ , respectively. The results of these tests are found in table 12.

Most of the exchange experiments have been performed on powdered materials. In those cases where single crystals could be grown either by Czochralski or flux evaporation, attempts were made to ion exchange the single crystals.

In general, the results of ion exchange experiments on single crystals were disappointing in that either disruption of the single crystal occurred or exchange proceeded at extremely low rates.

Ion exchange experiments were conducted in the $\text{Rb}_2\text{O-Nb}_2\text{O}_5$ system with particular emphasis on the "11-layer" compound occurring at or about 26.67 mol per cent Rb_2O . Ion exchange experiments were conducted on both single

Table 12a. Summary of Ion Exchange Experiments

Exchange Media	Temp °C	Time hrs	Results
$4\text{Rb}_2\text{O}:11\text{Nb}_2\text{O}_5$ ^{a/}			
<u>Single Exchange</u>			
KNO_3	400	3	K exch. "11-L" phase $\underline{a}=7.554$, $\underline{c}=43.398$
KNO_3	400	16	K exch. "11-L" phase
KNO_3	400	16	K exch. "11-L" phase
KNO_3	450	36	K exch. "11-L" phase
NaNO_3	500	1	Partially exch. $\underline{a}=7.4$, $\underline{c}=43.6$
NaNO_3	450	64	Partially decomposed
NaNO_3	414	17	Partially exch. $\underline{a}=7.458$, $\underline{c}=43.19$
NaNO_3	400	16	Partially exch. $\underline{a}=7.472$, $\underline{c}=43.23$
<u>Double Exchange</u>			
KNO_3	400	3	
NaNO_3	400	1.5	$\underline{a}=7.458$ $\underline{c}=43.398$
NaNO_3	400	16	$\underline{a}=7.368$ $\underline{c}=43.869$
KNO_3	400	16	
NaNO_3	450	66	$\underline{a}=7.366$ $\underline{c}=43.898$
KNO_3	400	16	
NaNO_3	450	98	$\underline{a}=7.332$ $\underline{c}=43.997$
$\text{Rb}_2\text{O}:3\text{Nb}_2\text{O}_5$			
<u>Single Exchange</u>			
KNO_3	450	3	K exch. "9-L" phase $\underline{a}=7.56$, $\underline{c}=36.52$
$21.75\text{Rb}_2\text{O}:78.25\text{Nb}_2\text{O}_5$ ^{a/}			
<u>Single Exchange</u>			
KNO_3	450	18	No exchange
KNO_3	450	99	
NaNO_3	450	99	Partial exch., increase in "c" and partial decomposition
<u>Double Exchange</u>			
KNO_3	450	18	
NaNO_3	450	23	Partial exch.
$\text{RbTa}_2\text{O}_5\text{F}$			
<u>Single Exchange</u>			
KNO_3	340	2.5	Partial exch. $\underline{a}=7.512$, $\underline{c}=3.879$
KNO_3	340	15	Partial exch. $\underline{a}=7.512$, $\underline{c}=3.879$
KNO_3	450	16	Partial exch. $\underline{a}=7.512$, $\underline{c}=3.879$
NaNO_3	340	3.5	No exchange
<u>Double Exchange</u>			
KNO_3	450	16	
NaNO_3	340	2	No exchange
KNO_3	450	16	
NaNO_3	450	44.5	Some decomposition, partial exchange $\underline{a}=7.51$, $\underline{c}=3.814$
$\text{Rb}_{1-5x}\text{Nb}_{3.4+x}\text{O}_9$			
<u>Single Exchange</u>			
NaNO_3	500	2	Unchange HTB+ $\text{Na}_2\text{Nb}_4\text{O}_{11}$ (tr) + NaNbO_3 (tr)
NaNO_3	330	2	No change
$3\text{NaNO}_2:2\text{NaNO}_3$	240	22	No change
KNO_3	500	2	KNbO_3 + unchange HTB

^{a/} Single crystal fragments

Table 12b. Summary of Ion Exchange Experiments with $4\text{Rb}_2\text{O}:\text{11Nb}_2\text{O}_5$ Pellets

Starting Material	Pressing History	Firing History	K^+ Exchange History	Na^+ Exchange History	Remarks
$4\text{Rb}_2\text{O}:\text{11Nb}_2\text{O}_5$ 500°C-90 hr ^{c/}	10000 psi ^{a/}	1200°-7 hr			Pellets cracked during firing $\underline{a}=7.522$ $\underline{c}=43.180$
	20000 psi ^{b/}		KNO_3 -20 hr @400° partial exchange ^{e/}		Pellet fragment disintegrated $\underline{a}=7.128$, $\underline{c}=43.469$
		↑15°/hr 1200°-7 hr	KNO_3 -16 hr @400° partial ex- change	NaNO_3 -18 hr @400°C Partial ex- change	Pellet fragment did not disintegrate K^+ $\underline{a}=7.575$, $\underline{c}=43.469$ Na^+ $\underline{a}=7.390$, $\underline{c}=43.663$
		↑5°/minute 1200°-1 hr ↓5°/minute	KNO_3 -1 hr @400° complete exchange		Pellet did not disintegrate K^+ $\underline{a}=7.545$, $\underline{c}=43.332$
		↑3°/minute 1200°-1 hr ↓3°/minute	KNO_3 -19 hr @400° complete exchange		Pellet displayed some spalling K^+ $\underline{a}=7.555$ $\underline{c}=43.428$
500-120 hr ^{d/} 600-90 hr ^{d/}	10000 psi ^{a/}	1100°-1 hr	KNO_3 -16 hr @400° complete exchange	NaNO_3 -21 hr @400°	K^+ $\underline{a}=7.551$, $\underline{c}=43.401$ Na^+ cells not calculated due to broadness of lines in diffraction
		1100°-1.5 hr	KNO_3 -16 hr @400° partial exchange	NaNO_3 -41 hr @400° partial exchange	Na^+ exchanged pellet decomposed K^+ $\underline{a}=7.547$, $\underline{c}=43.428$ Na^+ $\underline{a}=7.404$, $\underline{c}=43.332$
		1100°-1 hr	KNO_3 -72 hr @400° complete exchange	NaNO_3 -32 hr @400° partial exchange	K^+ $\underline{a}=7.557$, $\underline{c}=43.442$ Na^+ $\underline{a}=7.484$, $\underline{c}=43.482$
	10000 psi ^{a/} 20000 psi ^{b/}	1100°-1 hr 1200°-1 hr 1100°-16 hr 1200°-2 hr	KNO_3 -16 hr @400° complete exchange		Pellet cracked during final 1200° firing K^+ $\underline{a}=7.557$ $\underline{c}=43.442$
		↑5°/minute 1200°-5 hr ↓5°/minute	KNO_3 -2 hr @400° complete exchange		Powder fired in open tube K^+ $\underline{a}=7.549$, $\underline{c}=43.387$
			KNO_3 -18 hr ^{d/} @400° complete exchange	NaNO_3 -18 hr @400° complete exchange	K^+ $\underline{a}=7.553$, $\underline{c}=43.387$ Na^+ $\underline{a}=7.375$, $\underline{c}=43.830$

^{a/} pressed in steel dies^{b/} isostatic pressing^{c/} without PVA binder^{d/} with PVA binder^{e/} complete exchange

		a	c
$4\text{Rb}_2\text{O}:\text{11Nb}_2\text{O}_5$	=	7.522Å	43.180Å
K^+ exchanged product	=	7.554Å	43.398Å
Na^+ exchanged product	=	7.368Å	43.869Å

crystal fragments obtained from crystals grown from the melt and low temperature calcines of 4:11 powders. The single crystals underwent K^+ exchange in molten KNO_3 but disintegrated during Na^+ exchange in $NaNO_3$ during various temperature and time combinations. Pellets of the "11-L" phase were pressed both uniaxially and isostatically with and without polyvinyl alcohol binder, fired and x-ray diffraction powder patterns made before any attempt was made to exchange. Generally the K^+ exchange occurred without too much degradation of the specimen but the pellets disintegrated to a fine powder during Na^+ exchange. The unit cell dimensions for complete ion exchange (table 12) were developed from the results of ion exchange in molten salts from very small single crystal fragments.

3. Relation of Structural Mechanisms of Non-stoichiometry to Ionic Conductivity

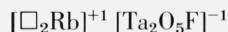
It is probably generally accepted that a phase which exhibits unusual ionic conductivity must necessarily be structurally non-stoichiometric. Unfortunately the opposite is not necessarily true. For this reason it is worthwhile to discuss the nature of the non-stoichiometry which has been observed in this study for those phases which seem to be of interest.

3.1. Hexagonal Tungsten Bronze-type Phases (HTB)

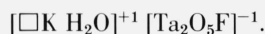
It has already been reported [2, 5] that the hexagonal tungsten bronze-type phase (HTB) found in binary alkali niobate and tantalate systems has alkali ions in non-stoichiometric positions and excess Nb^{+5} or Ta^{+5} ions. These excess pentavalent ions may well block the alkali ion conductivity as these hexagonal bronzes cannot be ion exchanged. There are two mechanisms that have proved effective in altering the ion exchange characteristics of the hexagonal tungsten bronze-type structures. One is to change the total alkali:other cation valence ratio by substituting W^{+6} for Ta^{+5} , for instance in the system $KTaO_3-WO_3$ [1]. The alternate to replacing Ta^{+5} ions with W^{+6} ions is to change the structure enough to allow ion exchange (see sec. 3.3).

3.2. Pyrochlore Phases

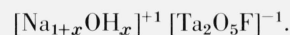
The pyrochlore structural formula should be written as $[A_2X][B_2X_6]$. The $RbTa_2O_5F$ is apparently equivalent to the formula



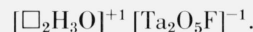
as shown by the structural study of single crystals [9] prepared by the flux synthesis method described by the present authors [2]. The Rb^+ ion is apparently too large for the A sites and it is this preference for the larger anion (X) site that makes this compound stable. During ion exchange in KNO_3 the K^+ ion apparently enters the A site and, upon exposure to atmospheric moisture, an H_2O molecule occupies the (X) site formerly containing Rb^+ . The formula is then



During sodium exchange it is apparently possible to obtain a non-stoichiometric amount of sodium in this lattice. The formula for this phase might be postulated as



The product obtained by acid leaching of this pyrochlore might then be



The differences in these formulas seem to be related to the size of the monovalent ions entering the ion exchangeable positions. Although infrared analysis of the Na^+ exchange product does not indicate $(OH)^-$ [9] it would probably be worthwhile to examine this product with NMR for hydrogen resonance, a much more sensitive method than infrared absorption.

3.3. Hexagonal Tungsten Bronze-Pyrochlore Series

The $[B_2X_6]$ framework of the pyrochlore structure can be described as consisting of alternating layers of the hexagonal tungsten bronze structure separated by layers of isolated octahedra sharing only two corners with the adjacent HTB layers. If this structure is modified by increasing the sequence number of either of these types of layers from the cubic packing of $AaBbCc$ to any other arrangement, a sequence of hexagonal phases would be formed having the same a axis as the HTB structure and with varying but integral multiplicities of the c axis dimension. Such phases are actually encountered in the $K_2O-Ta_2O_5$ [1], $Rb_2O-Nb_2O_5$ and $Rb_2O-Ta_2O_5$ [2] systems and had been estimated by us to represent "9-layer", "16-layer", and "11-layer" sequences. All of the phases can be ion exchanged by K^+ and Na^+ unlike the HTB phases in the same systems. The reason for this appears to be that a rotation or translation of a portion of the layer sequence allows the isolated vertical channels found in the HTB structure to be changed to intersecting channels as in the cubic pyrochlore structure. Unfortunately, however, the Na^+ ion exchanged products are not stable above about 450 °C.

As in the case with the pyrochlore compounds, the K_2O containing phases have unit cell dimensions very similar to or even larger than the corresponding Rb_2O containing phases (table 13). For instance the c axis for the "11-layer" phase in the $K_2O-Ta_2O_5$ system is 43.512 Å while that in the $Rb_2O-Nb_2O_5$ system is 43.18 Å and in the $Rb_2O-Ta_2O_5$ system it is 43.19 Å. This may be due to a real difference in total alkali content. It may also be due to hydration of the K_2O phases. No high temperature x-ray data is available to check this hypothesis but small single crystals of the 2:5 $K_2O:Ta_2O_5$ phase have been noted to crack, spall and jump on exposure to air.

A mechanism of structural chemistry applicable to these phases was first described by Gatehouse [10] for a crystal of a metastable phase prepared in this laboratory [1] in the $K_2O-Ta_2O_5$ system and called metastable $K_2O:3Ta_2O_5$. Gatehouse has shown that a rotation or translation of one layer of hexagonal bronze can fit into another so that a basic unit is formed with one set of three corner shared octahedra lying above a second set of three corner shared octahedra, each octahedra sharing two edges with the second set. The ideal

Table 13. Unit Cell Data for Phases Found in the Ta_2O_5 - $KTaO_3$, Nb_2O_5 - $4Rb_2O:11Nb_2O_5$, and Ta_2O_5 - $4Rb_2O:Ta_2O_5$ Systems.

System	Designation	Composition Mole %		Symmetry	Unit Cell Dimension				Conditions Limiting Possible Reflections	Probable Space Group
					a	b	c	β		
		Rb_2O	Nb_2O_5		\AA	\AA	\AA			
Rb_2O - Nb_2O_5	11-L	26.67	73.33	Hexagonal	7.522	-	43.18	-	hk ℓ : -h+k+l=3n	$R3, R\bar{3}, R32, R3m, R\bar{3}m$
	16-L	25.5	74.5	Hexagonal	7.514	-	65.12	-	hh ℓ : ℓ =2n	$P6_3mc, P\bar{6}2c, P6_3mmc$
	9-L	25	75	Hexagonal	7.518	-	36.353	-	hh ℓ : ℓ =2n	$P6_3mc, P\bar{6}2c, P6_3mmc$
	HTB	21.75	78.25	Orthorhombic	12.991	7.550	7.796	-	hk0: h+k=2n	Pmcn
	GTB	11.5	88.5	Tetragonal	27.484	-	3.9757	-	h0 ℓ : ℓ =2n h00: h=2n	$P42_12, P\bar{4}2_1m$
		Rb_2O	Ta_2O_5							
Rb_2O - Ta_2O_5	11-L	26.67	73.33	Hexagonal	7.506	-	43.19	-	hk ℓ : -h+k+l=3n	$R3, R\bar{3}, R32, R3m, R\bar{3}m$
	9-L	25	75	Hexagonal	7.508	-	36.41	-	hh ℓ : ℓ =2n	$P6_3mc, P\bar{6}2c, P6_3mmc$
	HTB	21.75	78.25	Hexagonal	7.531	-	3.907	-	none	$P6_3mmc$
	GTB	11.5	88.5	Tetragonal	27.573	-	3.9018	-	h00: h=2n	$P42_12, P\bar{4}2_1m$
		Ta_2O_5	K_2O							
Ta_2O_5 - $KTaO_3$	GTB	88.5	11.5	Tetragonal	27.55	-	3.899	-	h00: h=2n	$P42_12, P42_1m$
	1:5	83.33	16.67	Orthorhombic	5.654	10.713	16.80	-	h0 ℓ : ℓ =2n 0k ℓ : k=2n	$Pbcm, Pbc2_1$
	TTBs	80	20	Orthorhombic	12.547	37.641	3.922	-	h0 ℓ : h=2n	Pmam, $P2_1am$, Pma2
	HTB	78.25	21.75	Hexagonal	7.527	-	3.901	-	none	$P6mmm$
	9L	73.85	26.15	Hexagonal	7.55	-	36.583	-	hh ℓ : ℓ =2n	$P6_3mc, P\bar{6}2c, P6_3mmc$
	16L	73.5	26.5	Hexagonal	7.542	-	65.57	-	hh ℓ : ℓ =2n	" " " "
	11L	71.43	28.57	Hexagonal	7.54	-	43.512	-	hk ℓ : -h+k+l=3n	$R3, R\bar{3}, R32, R3m, R\bar{3}m$
	1:2	66.67	33.33	Hexagonal	6.283	-	36.878	-	hk ℓ : -h+k+l=3n	" " " " " "
	TTB	66	34	Tetragonal	12.569	-	3.957	-	h0 ℓ : h=2n	Pmam, $P2_1am$, Pma2
	3L*	75	25	Hexagonal	9.051	-	22.284	-	h0 ℓ : ℓ =2n	$P6_3cm, P\bar{6}c2, P6_3mcm$
	H-1:3*	75	25	Monoclinic	14.614	3.774	6.557	98°30'	none	$P2, Pm, P2/m$

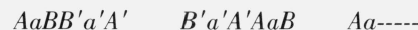
* Metastable phase obtained from quenched liquid.

composition of this structure was labeled $A_6B_{15.6}O_{42}$ or 27.78 per cent alkali rather than 25 per cent alkali. Ternary compounds isostructural with this phase were reported by Groult et al. [11], with the ideal formula $A_3M_8O_{21}$ or 27.27 per cent alkali.

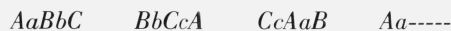
Specimens of the hexagonal niobates and tantalates from the Rb_2O and K_2O systems were given to Dr. Gatehouse of Monash University for single crystal x-ray diffraction structure determination [10] and to Dr. Yagi at Arizona State University for study by the ultra high resolution electron microscope lattice image technique [12]. Both of these studies indicate that the "9-L", "16-L", and "11-L" designations are misnomers. The designations "9-L", "11-L", and "16-L" should be dropped and a new nomenclature substituted. It is apparent that the "9-L" and "11-L" structures are made up of double hexagonal units of the type described by Gatehouse alternating with isolated octahedra and mirror (twinned) images of the two layers of the pyrochlore structure. The 16-L structure is an ordered intermediate between the other two phases.

Complete details of the lattice image and structure determinations will be published elsewhere, however, the basic principles are described here. The pyrochlore structure can be written as $AaBbCcAaBbCc \dots$ where A, B, and C are

the hexagonal bronze layers and a, b, c are the isolated octahedra. The structure of the "9-L" phase was described by Yagi [12] from the lattice image pictures as:



where the prime symbol denotes a mirror image (combined with translation or rotation). This can be described as a double block structure and has hexagonal symmetry. The "11-L" structure is:



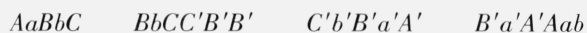
and can be described as a triple block structure with rhombohedral symmetry. Note that in the double block structure ("9-L") each block contains two mirrored "twins" whereas no such mirror "twins" exist in the triple block ("11-L") structure. The ideal basic "9-L" block is:

$$(Aa+B) + (B'a') + 1/2A' = (6+4) + (6) + (2) = 18 \text{ \AA}$$

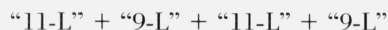
where the basic "11-L" block is:

$$(Aa) + (Bb) + 1/2C = (6) + (6) + (2) = 14 \text{ \AA}$$

The "16-L" phase is an ordered intermediate which is hexagonal and contains two of each type of block. It is therefore a four block phase and has the structure:



or



or

$$2(18+14) = 2(32) = 64\text{\AA}.$$

4. Conclusion

Several different structure types were found to be present in the two subsystems examined. The hexagonal bronze stacking sequence similar to that found in the $K_2O-Ta_2O_5$ system was found to be present as well as the Gatehouse bronze found in the $K_2O-Nb_2O_5$ system. Ion exchange reactions proved that suitable structure types could be easily K^+ ion exchanged but Na^+ ion exchange lead to excessive volume change and destruction of both ceramic specimens and single crystals. Melt and flux growth yielded single crystals of the HTB, GTB, and the triple block rhombohedral phase in the $Rb_2O-Nb_2O_5$ system. In the $Rb_2O-Ta_2O_5$ system, single crystals of the large double block hexagonal phase were grown by the flux evaporation method.

It should be emphasized that the explanation of the crystal chemistry of these phases is due to the cooperation between three separate and distinct groups. This laboratory contributed the syntheses, phase equilibria, unit cell dimensions, and alkali metal oxide ratio. Dr. Gatehouse and his group at

Monash University, Clayton, Australia contributed the first solution to the crystal structures and the crystal structure refinements, while Dr. Yagi of the Tokyo Institute of Technology, while a guestworker at Arizona State University, contributed the lattice image studies and their final interpretations as hexagonal bronze-pyrochlore mixtures.

We would like to also give credit to Dr. S. Andersson of Lund Institute of Technology, Sweden, and to Dr. J. Galy of CNRS, Toulouse, France for first pointing out the possibility of this hexagonal bronze-pyrochlore stacking sequence.

5. References

- [1] Roth, R. S., Parker, H. S., Brower, W. S., and Minor, D. B., Alkali Oxide-Tantalum Oxide and Alkali Oxide-Niobium Oxide Ionic Conductors, NASA Report No. CR-134599, April 1974.
- [2] Roth, R. S., Brower, W. S., Parker, H. S., Minor, D. B., and Waring, J. L., Alkali Oxide-Tantalum, Niobium and Antimony Oxide Ionic Conductors, NASA Report No. CR-134869, April 1975.
- [3] Riesman, A., and Holtzberg, F., J. Phys. Chem. **64**, 748 (1960).
- [4] Iyer, P. N., and Smith, A. J., Acta. Cryst. **B27**, 731 (1971).
- [5] Gatehouse, B. M., Lloyd, D. J., and Mishkin, B. K., Solid State Chemistry, Proceedings 5th Materials Research Symposium, NBS Special Publ. **364**, 15 (1972).
- [6] Powell, R. L., Hall, W. J., Hyink, C., Jr., Sparks, L. L., Burns, G. W., Scroger, M. G., and Plunb, H. H., Thermocouple Reference Tables Based on the IPTS-68, NBS Monograph **125**, 4 (1974).
- [7] Roth, R. S., Parker, H. S., Brower, W. S., and Waring, J. L., Fast Ion Transport in Solids, Solid State Batteries and Devices, Ed. W. vanGool, Proceedings of the NATO Sponsored Advanced Study Institute, Belgrate, Italy, September 1972 (North Holland Publishing Co., Amsterdam, 1973), pp. 217-232.
- [8] Brower, W. S., Minor, D. B., Parker, H. S., Roth, R. S., and Waring, J. L., Matls. Res. Bull. **9**, 1045 (1974).
- [9] Goodenough, J. B., Y-P Hong, H., Kafalas, J. A., Dwight K., Jr., Research for Preparation of Cation Conducting Solids by High Pressure Synthesis and Other Methods, NASA Report No. C-43205-C/PR/75, March 1975.
- [10] Gatehouse, B. M., J. Less Common Metals **50**, 139-144 (1976).
- [11] Groult, D., Chailleux, J. M., Choynet, J., and Raveau, B., J. Solid State Chem. **19**, 235-244 (1976).
- [12] Yagi, K., Personal communications, 11/3/76, 11/24/76, 12/28/76.